Applied Physics Letters

Perspective on room-temperature solid-state masers

Cite as: Appl. Phys. Lett. **119**, 140502 (2021); https://doi.org/10.1063/5.0061330
Submitted: 25 June 2021 • Accepted: 17 September 2021 • Published Online: 08 October 2021

Daan M. Arroo, Neil McN. Alford and Jonathan D. Breeze

Applied Physics Letters PERSPECTIVE scitation.org/journal/apl

Perspective on room-temperature solid-state masers

Cite as: Appl. Phys. Lett. **119**, 140502 (2021); doi: 10.1063/5.0061330
Submitted: 25 June 2021 · Accepted: 17 September 2021 ·
Published Online: 8 October 2021

Daan M. Arroo,[1,2] Neil McN. Alford,[1,2] and Jonathan D. Breeze[3,4,a)]

AFFILIATIONS

[1]Department of Materials, Imperial College London, Exhibition Road, London SW7 2AZ, United Kingdom
[2]London Centre for Nanotechnology, Imperial College London, Exhibition Road, London SW7 2AZ, United Kingdom
[3]Department of Physics and Astronomy, University College London, Gower Street, London WC1E 6BT, United Kingdom
[4]London Centre for Nanotechnology, 17-19 Gordon Street, London WC1H 0AH, United Kingdom

[a)]Author to whom correspondence should be addressed: j.breeze@ucl.ac.uk

ABSTRACT

The first solid-state masers to operate at room-temperature and ambient air-pressure were recently demonstrated using optically pumped spin-triplet states as the gain medium. In this Perspective, we briefly review the previous state-of-the-art in cryogenic solid-state masers and then discuss the development of the room-temperature solid-state maser: from the organic pentacene pulsed maser to the diamond nitrogen-vacancy continuous-wave maser. We characterize the operation of these masers as coherent microwave sources and ultra-low noise amplifiers before outlining how they can be adapted to act as model systems in which to explore room-temperature cavity quantum electrodynamics. After discussing challenges facing current embodiments of the room-temperature solid-state maser, we explore how they might be addressed or by-passed altogether through the development of alternative materials and masing mechanisms. Finally, we speculate on how the advent of masers that can operate in ambient conditions might lead to novel applications in metrology and quantum technologies.

I. BACKGROUND

The maser is the microwave analog of the laser, employed in communications and radio astronomy due to its ability to amplify microwave signals with exceptionally low levels of noise. Using atomic beams, vapors, or defects in solid-state systems as gain media, population inversions allow the stimulated emission of high-intensity, coherent radiation from excited states.

The theoretical principles underpinning the operation of the MASER (microwave amplification by stimulated emission of radiation) were first proposed independently by Weber[1] and by Basov and Prokhorov[2] in the early 1950s. This led to the first working maser, based on ammonia, being demonstrated in 1954 by Gordon *et al.*[3] Following this demonstration, there was a period of rapid development with work on atomic masers culminating in the demonstration of the hydrogen maser in 1960.[4,5]

In parallel to the work on atomic masers, Bloembergen launched an equally fruitful wave of investigations into solid-state masers by proposing a simple three-level system in 1956.[6] This led to the development of relatively compact solid-state masers based on paramagnetic salts and Cr^{3+} impurities in ruby[7–10] that quickly found applications in radar[11] and radio astronomy, where it facilitated the first measurement of the (surprisingly high) temperature of Venus.[12,13]

The laser, first reported by Maiman in 1960[14] as an optical version of the maser, went on to enable many innovations in spectroscopy, manufacturing, communications, medicine, and metrology. The maser, however, was compromised by the challenging experimental conditions required for its operation. Atomic[15] and free-electron masers[16] require ultra-high vacuum with associated bulky equipment such as chambers and pumps to achieve and maintain population inversion. In contrast, certain optically pumped solid-state masers[17] could escape the requirement for ultra-high vacuum but still needed cryogenic refrigeration, strong magnetic fields, and magnetic shielding. The key barrier of requiring cryogenic temperatures was particularly difficult to overcome since in order to achieve significant population inversions in solid-state systems, either the energy gap of the maser transition should significantly exceed the system temperature ($\hbar\omega_\mu \gg k_B T$), so that there is a large ground-state population to pump, or the spin-lattice relaxation rate must be slow enough to allow an appreciable excited-state population to build up. Since for any microwave

transition ($\lambda > 1$ mm), the transition energy must satisfy $\hbar\omega_\mu < 14.4$ K and the spin-relaxation rate increases sharply with temperature, this typically rules out maser operation at room temperature. For these reasons, soon after the discovery of the maser, attention switched to the laser and newly discovered semiconductor devices, whose larger energy gaps allowed them to operate at room-temperature and in Earth's magnetic field. As research focused on lasers, masers found application only in niche areas where their ultra-low noise amplification was essential such as radio astronomy[12] and frequency standards.[18] Given the ubiquity of microwave devices in modern communications infrastructure, it is nevertheless interesting to consider in greater detail the technological barriers that prevented masers from gaining the widespread adoption of lasers.

The cornerstone of both masers and lasers is the gain medium which, through a variety of pumping schemes (including electrical,[19] chemical,[20] optical,[21] and state selection[22]) requires the population of two of its energy levels to be inverted—a higher energy state is more populated than a lower energy state. Through stimulated emission, the photon population within a maser or laser resonant cavity or wave-guiding structure can grow exponentially at a rate exceeding any photon loss mechanisms, thus coherently amplifying any input photons with high gain and low-noise or providing a coherent source of radiation.

Atomic masers, such as the hydrogen maser, can operate at room-temperature, but their output power is weak due to the typically low hydrogen density and inefficient state selection.[22] They are also complex to engineer: gaseous H_2 is disassociated into atomic hydrogen via radio frequency plasma discharge then fed through a state selector and finally into a PTFE (polytetrafluoroethylene)-coated high quality-factor microwave cavity resonant with the frequency of the hydrogen emission line at 1.42 GHz. Traditional solid-state masers employ a multi-level pumping scheme, the simplest consisting of three levels as proposed by Bloembergen. The transition between the lowest and highest levels is saturated by a microwave pump, establishing a population inversion between the highest state and a less populated intermediate state [Fig. 1(a)]. To make the pump process more efficient, cryogenic cooling with liquid helium to a temperature ~4 K is necessary to increase the relative population of the lowest state according to Boltzmann statistics, from which the levels are populated as $n_{\text{low}}/n_{\text{high}} = \exp(\hbar\omega_\pi/k_B T)$ at equilibrium where $\hbar\omega_\pi$ is the energy gap between the lowest and highest levels. This pumped three-level system operating at cryogenic temperatures forms the basis of state-of-art solid-state masers such as the ruby maser [Cr-doped Al_2O_3, Fig. 1(b)]. Alternatively, increasing the pump frequency ω_π to millimeter-wave and even up to optical frequencies can further increase the inversion. Nevertheless, cryogenic operation has remained necessary for masers based on paramagnetic impurities, such as Cr^{3+} and Fe^{3+}, in ruby even where large ground-state populations can be achieved at higher temperatures, because the transverse spin decoherence rates and longitudinal spin-lattice relaxation rates are too rapid at room-temperature, enhanced by the immersion of the impurities within a spin-bath of Al^{3+} ions with nuclear spin $I = 5/2$ and spin-phonon interactions such as two-phonon Raman scattering with a T^7 to T^9 temperature dependence.

A more recent update on the three-level solid state maser exploited the very high quality factors ($Q > 10^9$) that can be achieved in whispering-gallery mode resonators at low temperatures.[23] By designing a sapphire resonator so that one of its whispering gallery modes had a frequency coincident with the 12.04 GHz zero-field EPR transition between the $|1/2\rangle$ and $|3/2\rangle$ states of Fe^{3+} impurities in the sapphire and pumping the $|1/2\rangle \leftrightarrow |5/2\rangle$ transition at 31.3 GHz, Bourgeois *et al.*[24] demonstrated successful maser oscillation. The whispering-gallery maser oscillator was subsequently developed further[25,26] to achieve power outputs as high as 2.5 nW—four orders of magnitude beyond the power output achieved with hydrogen masers.[27] Since the Schawlow–Townes limit[28] on the frequency stability depends inversely on the output power, this makes these systems

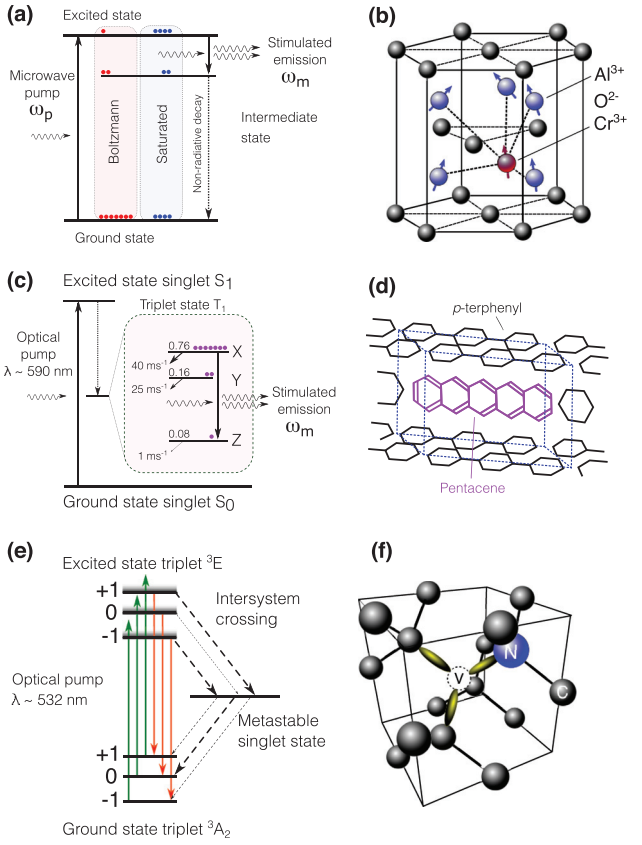

FIG. 1. Jablonksi diagrams and crystal structures of maser gain media. (a) A generic three-level pumping scheme. A population inversion (blue) relative the Boltzmann population (red) is achieved by using microwave pumping to promote electrons from the ground state to an excited state of energy $\hbar\omega_\pi$, from which masing occurs at frequency ω_μ by stimulated transitions to an intermediate state. (b) Crystal environment of a Cr^{3+} impurity ruby in Cr-doped Al_2O_3, used in state-of-the-art ruby masers. (c) Pumping mechanism for the pentacene maser. Electrons in pentacene molecules are efficiently pumped from the ground-state singlet into long-lived metastable triplet states through photoexcitation and intersystem crossing, leading to a population inversion between the *X* and *Z* triplet-state sub-levels. (d) A pentacene molecule in the para-terphenyl crystal environment used as a gain medium for the pentacene maser. (e) Pumping scheme for the diamond maser. By applying an external magnetic field along the nitrogen-vacancy center (NV) axis, the energy of the triplet $S = -1$ state is pushed below that of the spin-singlet state by Zeeman splitting, allowing an inversion to be achieved through spin-selective intersystem crossing. (f) Crystal environment of a NV center in diamond, used as a gain medium in the diamond maser.

highly promising as frequency standards with a potential frequency stability of order $10^{-16}\tau^{-1/2}$, where τ is the integration time. Nevertheless, while the whispering-gallery maser oscillator operates at zero-field, it still relies on cryogenic (< 5 K) temperatures to achieve the inversion and low dielectric losses required to operate.

The capacity for solid-state masers to operate as compact, high-output, and low-noise microwave amplifiers was, thus, well-established with a final obstacle to broader employment in microwave devices being the necessity for cryogenic temperatures.

II. REVIEW OF ROOM-TEMPERATURE MASERS

In 2012, the first solid-state maser to operate at room-temperature was reported,[29] using photoexcited triplet-states in organic pentacene molecules as the gain medium. This discovery can be traced back to earlier work on microwave dielectric ceramics. These materials, used in microwave communications, rely on three key properties—relative permittivity ε_r, dielectric loss tan δ, and temperature coefficient of permittivity τ_ε. The development of a distributed Bragg-reflector resonator[30] analogous to a photonic crystal, constructed from concentric cylindrical sapphire rings and plates but departing from conventional quarter-wave thicknesses, demonstrated a Q-factor of 6×10^5 at 30 GHz.[31,32] The question was posed of what other applications could be found for such a high Q-factor at room-temperature instead of the obvious: the frequency discriminating component of low phase-noise oscillators and frequency standards.

The idea of using photoexcited triplet-states in organic molecules as maser gain media had previously been proposed by Brock *et al.*[33] in 1961 who wrote that "coherent stimulated emission at microwave or millimeter wavelengths may prove feasible using the population in the Zeeman levels of the first triplet state. Such an emission process would permit the realization of organic molecular crystal masers having the unique property of being active only when optically excited." This proposal was pursued experimentally by Blank *et al.*[34–36] using inverted populations within photoexcited triplet-state sub-levels of organic paramagnetic molecules. In an ensemble of C_{60} dissolved in toluene they observed[34] spin-lattice relaxation times of $T_1 \sim 10$ μs at 253 K, leading them to conclude that the triplet mechanism was incapable of generating sufficiently long coherence times for maser operation. Subsequent work took place on a solution of trityl radicals and etioporphyrin triplets with a more complicated inversion process, in which photoexcited triplets led to chemically induced population inversion in the radicals,[20,37] allowing the spin-lattice relaxation time to be extended further to $T_1 \sim 100$ μs at room temperature.[35] However, Blank and Levanon were ultimately not able to overcome cavity losses sufficiently to allow their triplet-radical system to operate as a maser.[36]

To realize the first room-temperature solid-state maser, Oxborrow *et al.* doped a single-crystal of para-terphenyl with 0.01% of pentacene to produce the gain medium [Fig. 1(d)]. Through photoexcitation and intersystem crossing (ISC), electrons in singlet ground-states within pentacene molecules can populate long-lived (mean lifetime ~45 μs) metastable triplet states with a high quantum yield of ~65%.[38] Intramolecular electronic dipole-dipole interactions at zero magnetic field lift the degeneracy of the triplet sub-level energies, resulting in three non-degenerate sub-levels, X, Y, and Z, in the order of decreasing energy, populated in the ratio 9.5:2:1 as shown in Fig. 1(c). The maser exploited a population inversion between the X and Z triplet-state sub-levels with an energy difference equivalent to approximately 1.45 GHz. The pentacene:para-terphenyl crystal was placed within the bore of a cylindrical sapphire ring which formed part of a microwave cavity supporting a $TE_{01\delta}$ mode with resonant frequency matching the X–Z transition at 1.45 GHz and unloaded Q-factor 180 000. The magnetic energy distribution of the $TE_{01\delta}$ mode has an antinode at the center of the sapphire ring, where there is an axial magnetic dipole that induces transitions between the X and Z sub-levels when it is aligned with the molecular y-axis of pentacene. The pentacene molecules were optically pumped by a pulsed dye laser with wavelength ~585 nm and duration 1 ms, resulting in a maser emission burst of duration 450 μs [Fig. 2(a)]. The optical pump threshold power was determined to be about 230 W with a peak microwave power output of −10 dBm—100×10^6 times greater than the hydrogen maser—achieved when the pump power was increased further.[29]

The pentacene maser was subsequently miniaturized by replacing the sapphire (Al_2O_3) dielectric resonator material with a relative

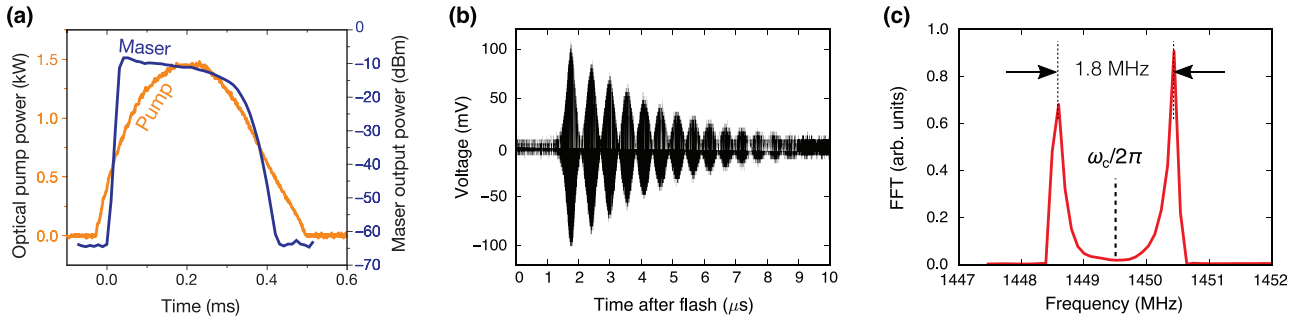

FIG. 2. Operation of a pulsed pentacene:para-terphenyl maser and observation of Rabi oscillations and mode-splitting, indicating that the system can operate in the strong-coupling regime of cavity quantum electrodynamics. (a) Pentacene maser trace showing the instantaneous pump power (yellow) and the output power measured over a 10 MHz band centered on 1.45 GHz (blue). Over the course of the 450 μs pulse, the pump laser delivers 0.5 J of energy to achieve an instantaneous output power of around −10 dBm. (b) Microwave output of a pentacene maser in a $SrTiO_3$ cavity after a single 15 mJ optical pulse. After a short delay during which spin–spin correlations and spin-photon coherence build up, Rabi oscillations are observed through an oscillatory microwave burst with a duration of around 10 μs. (c) Fourier analysis of the pentacene maser signal for a $SrTiO_3$ cavity with $\omega_c = 2\pi \times 1.4495$ GHz and 15 mJ optical pulse energy, showing split normal modes with a Rabi frequency of $\Omega \sim 2\pi \times 1.8$ MHz. The splitting was found to vary with the number N of excited pentacene molecules as $\sqrt{N}$, in agreement with the Tavis–Cummings model. [(a) Adapted from Oxborrow *et al.*[29] and [(b) and (c)] adapted from Breeze *et al.*[39]].

permittivity of $\varepsilon_r \approx 9$, by strontium titanate ($SrTiO_3$) with relative permittivity $\varepsilon_r \approx 318$, resulting in over two orders of magnitude reduction in the mode volume,[40] which scales with the permittivity as $V_m \propto \varepsilon_r^{-3/2}$. Although the $SrTiO_3$ resonator had a lower unloaded Q-factor of ~8000, it was nevertheless possible to achieve maser action due to the increased rate of stimulated emission resulting from the increased density of photonic states in the cavity, known as Purcell enhancement[41] and characterized by the Purcell factor $\mathcal{F}_P \propto Q/V_m$. The miniaturized maser produced a microwave pulse of stimulated emission when optically pumped by a xenon flashlamp with 70 W peak power and an estimated pump threshold power of ~20 W. Further work on this device, using nanosecond laser pulses enabled the temporal response of maser emission to be measured as a function of optical excitation energy and explained using the Lotka–Volterra (predator-prey) model,[42] recently interpreted as an example of superradiance.[43] A pentacene:para-terphenyl sample with increased concentration of pentacene revealed an unexpected phenomenon under nanosecond optical pumping—vacuum Rabi oscillations and normal-mode splitting[39] [Figs. 2(b) and 2(c)], indicating that the device was operating in the strong-coupling regime of cavity quantum electrodynamics (cQED). Strong-coupling is generally assumed to occur when the normal-mode splitting Ω is greater than both spin and photon mode decay rates but is more accurately defined as when it exceeds the mean of the spin decoherence/dephasing and cavity decay rates, $\Omega > \frac{1}{2}(\kappa_s + \kappa_c)$, where $\kappa_s = 2/T_2^*$ is the spin dephasing rate with T_2^* the dephasing time, and $\kappa_c = \omega_c/Q$ is the cavity decay rate where ω_c is the angular frequency of the cavity resonance and Q is its quality-factor. The normal-mode splitting for an ensemble of spins is given by $\Omega = 2g_e$, where g_e is the collective spin-photon coupling, itself proportional to the single spin-photon coupling $g_e = g\sqrt{N}$, where N is the number of spins or quantum emitters. The single spin-photon coupling is given by $g = \gamma_e\sqrt{\mu_0\hbar\omega_c/2V_m}$, where γ_e is the electron gyromagnetic ratio, μ_0 is the permeability of free space, and V_m is the magnetic mode volume.[39] Strong-coupling was achieved in the STO:pentacene maser by increasing the number of spins to $N \sim 10^{14}$ by increasing the concentration of pentacene molecules to ~0.1% and boosting the spin-photon coupling by reducing the mode volume to $V_m \sim 0.25$ cm^3. A key parameter in cQED is the "cooperativity" $C = 4g^2N/\kappa_s\kappa_c$, a figure of merit for the efficiency of coherent quanta transfer between different systems, in this case, a spin ensemble and a microwave cavity. The cavity contributes a factor $g^2/\kappa_c \sim Q/V_m$ to the cooperativity, which is proportional to the Purcell factor[41] and again reflects the relative density of photonic states.

To date, maser action in the pentacene-based system has only been observed for brief durations, typically of the order of milliseconds.[44] This is mainly due to two factors: (i) the relatively long lifetime of Z, the lowest triplet-state sub-level, reduces the number of pentacene molecules available for optical pumping, creating a "bottleneck" that quenches the population inversion and (ii) the organic gain medium host (para-terphenyl) cannot withstand continuous optical pumping due to its poor thermal conductivity and low melting point. Recent measurements of the spin-lattice relaxation and triplet-singlet decay rates[45] have revealed that rapid spin-lattice relaxation between the Y and Z sub-levels can lift the bottleneck, but gain medium heating is still an obstacle. Alternatively, it has been suggested[46] that replacing pentacene with other polyacenes, especially molecules based on anthracene and tetracene, is a promising route to continuous-wave masing, though this approach would rely on finding suitable host crystals to fill the role that para-terphenyl plays in the pentacene maser. Even with continuous-wave operation of the pentacene maser yet to be achieved, pulsed masing at room temperature and using only the Earth's magnetic field opens new avenues of investigation, and there will undoubtedly be further developments in this area.

Outside of organic gain media, attention in the pursuit of continuous-wave maser action at room temperature was naturally drawn to the long coherence times observed for spin defects in wide-bandgap materials.[47] Charged nitrogen-vacancy (NV) color centers in diamond [Fig. 1(f)] have ground-state triplets ($S = 1$) with remarkably long spin-lattice relaxations times ($T_1 \sim 5$ ms), (inhomogeneous) spin dephasing times ($T_2^* \sim 0.1$ μs), and (homogeneous) spin decoherence times ($T_2 \sim 10$ μs) at room-temperature. At zero magnetic field, the ground-state triplet consists of a pair of quasi-degenerate sub-levels $|\pm1\rangle$ at an energy $h\cdot$ 2.87 GHz above the $|0\rangle$ sub-level. NV centers have been the subject of intense research due to their spin-dependent photoluminescence (PL), allowing spin states to be initialized and readout optically. The $|0\rangle$ triplet sub-level can be preferentially populated by pumping the NV centers with green (~532 nm) laser light, resulting in a spin-polarized multi-level system. This occurs through spin-selective intersystem crossing of electrons from the photoexcited triplet state $|\pm1\rangle$ sub-levels into a metastable singlet-state, which then mostly decay into the ground-state triplet sub-level $|0\rangle$ [Fig. 1(e)].

The idea of using charged nitrogen-vacancy (NV) defects in diamond as a gain medium for room-temperature masers was first proposed in 1977 by Loubser and Van Wyk[48] and studied in more detail recently by Jin *et al.*[49] If an external magnetic field is applied along a $\langle111\rangle$ crystal axis direction, collinear with an NV axis, the $|\pm1\rangle$ sub-level energies split via the Zeeman interaction, leaving the $|0\rangle$ sub-level energy unchanged. If the field applied is greater than the zero-field splitting D-parameter (2.87 GHz or 102.5 mT), the $|-1\rangle$ sub-level energy drops below the populated $|0\rangle$ sub-level, resulting in a population inversion.

To achieve maser oscillation, the threshold pump rate per spin-defect can be shown[50] to be equal to $w_{thr} = \gamma/\Lambda(C-1)$, where $\Lambda < 1$ is a pump efficiency parameter that accounts for the likelihood of an electron being promoted into the $|0\rangle$ sub-level and γ is the spin-lattice relaxation rate. Having a cooperativity $C \geq 1$ is, therefore, a necessary condition for masing to be feasible. Considering the ideal situation of the pump efficiency being unity $\Lambda = 1$ and a cooperativity much greater than unity $C \gg 1$ reveals a counter-intuitive observation, that the pump threshold per spin defect is less than the spin-lattice relaxation rate, i.e., $w_{thr} \sim \gamma/C$. This occurs because the inversion per spin is clamped to $\sigma^z = 1/C$ above threshold, so only this fraction of the total number of spins participates in the maser action. This shows that the cooperativity C is also a measure of the collective nature of the maser process.

The first continuous-wave room-temperature solid-state maser was demonstrated in 2018 using NV^- color centers in diamond[50] (Fig. 3). The diamond, a 2 mm cube grown by chemical vapor deposition, was supplied by Element Six and contained ~4×10^{13} NV centers. The NV spin properties were characterized using pulsed and continuous electron spin resonance (ESR) spectroscopy at 9.2 GHz, yielding a spin-lattice relaxation time $T_1 = 4.8$ ms, spin decoherence time $T_2 = 22$ μs, and spin dephasing time $T_2^* = 0.5$ μs. A sapphire-dielectric loaded microwave resonator was designed with an optimized

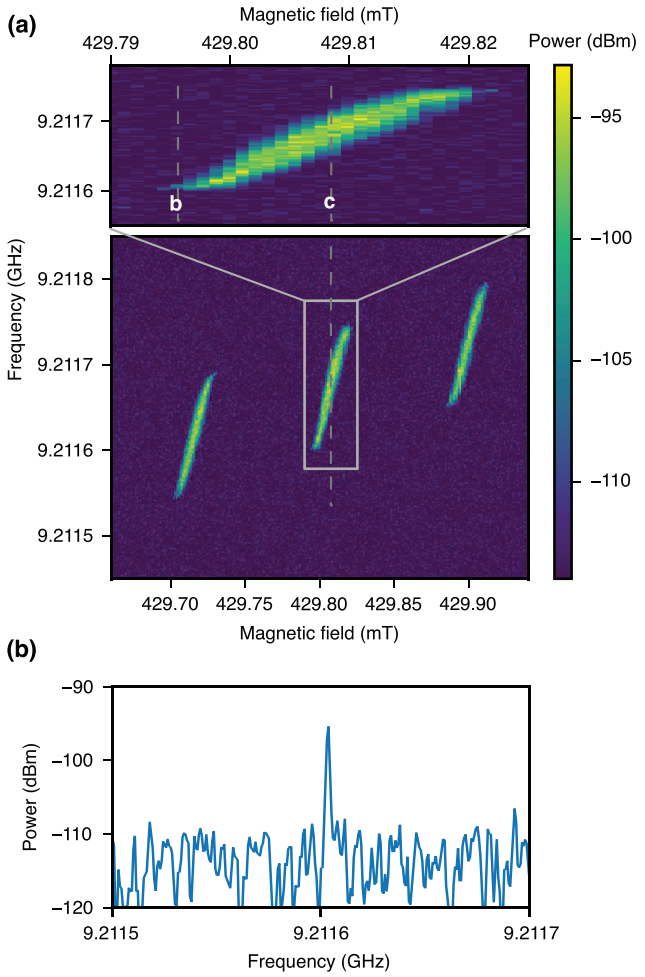

FIG. 3. Output power of the diamond maser as a function of the magnetic field and the microwave pump frequency with an optical pump power of 400 mW. (a) The system shows three regions of maser oscillation, corresponding to hyperfine transitions in the diamond nitrogen-vacancy centers. The white trace shows the power integrated over the frequency range at each field.[50] The central emission region (magnified at the top of the figure) shows a narrow (∼50 Hz) linewidth at its edges (b) in agreement with the Schawlow–Townes limit of ∼10 Hz, though at its center the peak is broadened due to limit cycles in the inversion-photon-population phase space. Adapted from Breeze *et al.*

Purcell factor $\mathcal{F}_P \propto Q/V_m$ with a loaded Q-factor of 30 000 (unloaded 55 000) and a magnetic mode volume V_m of 0.15 cm^3. Combined with the diamond sample, this system yielded a cooperativity $C \approx 11$. With an externally applied magnetic field of 430 mT aligned with one of the four ⟨111⟩ axes of the diamond and a modest 400 mW of optical pump power at 532 nm supplied by a Nd:YAG frequency-doubled laser, continuous maser emission was observed at 9.2 GHz with a peak power of −90 dBm (comparable with a hydrogen maser) and linewidth 50 Hz which agreed with the Schawlow–Townes limit of 10 Hz [Fig. 3(b)]. The mean pump rate per NV$^-$ center was estimated to be $w = 410$ s^{-1}. Scanning the magnetic field in small increments of 1 μT revealed three emission peaks separated by ∼2.7 MHz (∼0.1 mT), due to the hyperfine interaction of the NV$^-$ electron spin with the ^{14}N (I = 1) nucleus. ESR measurements confirmed a predicted inversion per NV center of $\sigma^z = 0.1$, corresponding to a negative spin-temperature of $|T_s| = 2.1$ K. This spin temperature represents the intrinsic noise temperature that may be expected when operating the diamond maser as a microwave amplifier and is comparable to the ∼1 K noise temperatures found in state-of-the-art ruby masers. However, by optimizing the cavity coupling and material properties of the diamond, it is expected that the noise temperatures could be reduced by a further order of magnitude to $|T_s| \sim 0.1$ K in ambient conditions.[49,51] Such low noise temperatures suggest that diamond masers will become especially valuable for applications, in which low phase noise is essential such as radar.

Before practical devices based on the diamond maser can be developed, there are certain challenges that must be overcome. The applied magnetic field needs to be highly uniform across the diamond sample to prevent inhomogeneous broadening of the NV center spin transition—for example, a 10 part-per-million inhomogeneity in the field at 430 mT would result in an additional 0.8 MHz increase in the spin dephasing rate κ_s. The temperature stability of any magnets employed will also be an important factor in this regard. Halbach arrays of rare-earth permanent magnets have been shown to provide fields of this magnitude with a high degree of homogeneity,[52] but variance in the properties of permanent magnets necessitates careful shimming of the magnet arrays. There is also the issue of sensitivity to extrinsic and intrinsic sources of magnetic noise, which could explain the observed instability of the emission line for zero spin-cavity detuning. For a linewidth of 0.1 Hz, the sensitivity of the maser frequency to magnetic fields is of the order of 10 pT/$\sqrt{\text{Hz}}$. Meanwhile, naturally abundant ^{13}C nuclei (1.2% of carbon atoms) and nitrogen donor impurities (P1 centers), the latter with typical concentrations in the region of 1–100 ppm depending on the diamond sample, will form significant sources of intrinsic magnetic noise.[53,54]

III. CHALLENGES AND FUTURE DEVELOPMENTS

While the realization of a diamond maser that operates at room temperature is a significant step toward broader technological adoption of masers, there remain certain challenges that must be overcome before broadly applicable devices become a reality. The most important of these are softening the requirement for a strong, spatially and temporally homogeneous magnetic field and reducing the effect of temperature fluctuations due to heating from the pump laser, while improving the efficiency with which the pump power is converted to output power (Jin *et al.*[49] suggest that it should be possible to attain output powers exceeding −50 dBm with an absorbed pump power of 1 W) and reducing the size of the cavity are further important steps. The latter two challenges might be addressed by fine-tuning the diamond crystal composition[51] and by using dielectric cavities with a high relative permittivity to reduce the mode volume and required pump power.[40]

For the other hurdles, it is worth exploring whether masers based on different operating principles might offer advantages. One such approach might exploit the exquisite control over the quantum states and the long coherence times of NV centers in diamond to prepare the spins in a coherent superposition of two energy levels, $|a\rangle$ and $|b\rangle$, whose transitions to a third state $|c\rangle$ are coupled to a detuned pair of lasers, giving transition probability amplitudes A_{ca} and A_{cb}. Since for absorption, the transition is from a coherent superposition to a

common final state, the amplitudes are summed before squaring and can destructively interfere. In contrast, amplitudes of stimulated emission from $|c\rangle$ to $|a\rangle$ or $|b\rangle$ are summed in square $|A_{ca}|^2 + |A_{cb}|^2$ so cannot cancel each other out. In this way, it is possible to achieve stimulated emission of coherent light even from relatively small populations of spins excited to $|c\rangle$, known as *lasing without inversion* (LWI).[55,56] This inversionless approach has already been realized in lasers with atomic vapors as gain media[57–60] and would remove the requirement for high pump powers necessary to achieve inversion. The demonstration of zero-field coherent population trapping for NV centers in diamonds strained along the [100] direction[61] suggests that this approach could also eliminate the need for an external magnetic field.

Another operating principle that might reduce the sensitivity of the emission frequency to thermal fluctuations in the gain medium is to develop masers based on superradiant emission,[43,62] in which stimulated emission from independent NV centers is replaced by coherent spontaneous emission from a collective excitation of the entire ensemble. This process may be qualitatively understood within the Dicke model,[63,64] which describes a system of N two-level atoms interacting with a single mode of the radiation field. When the strength of the atom-field interaction significantly exceeds the energy of the electromagnetic mode and the energy difference of the two atomic energy levels, there is a spontaneous phase-locking of the atomic dipoles. In this superradiant state, a large number of electromagnetic excitations are stored coherently in the atoms rather than in the radiation field and the system rapidly radiates with an intensity proportional to N^2.

Experimentally, the collective states required for superradiance are achieved by allowing emitters to interact with a single cavity mode in the "bad cavity" regime, where the cavity-mode decay rate is much faster than the rate at which emitters decohere or dephase. Since in such states information about the phase and amplitude is stored in the ensemble of emitters, the superradiant emission becomes insensitive to small fluctuations in the cavity length that might lead to the dephasing of optical modes and has been used as the basis for ultrastable superradiant lasers,[65,66] in which a repumping laser maintains the collective excited state to allow continuous superradiant emission. Since superradiance has already been observed from diamond NV centers at low temperatures[67,68] and it has been demonstrated in the pentacene-based system that the collective spin-photon states required can be generated[39] even at room temperature (with possible signs of superradiance[42,43]), it seems likely that a similar tactic may stabilize diamond-based room-temperature masers against thermal fluctuations in the cavity. A recent theoretical study[69] further suggests that if diamond NV center-based superradiant masers are realized, it should be possible to reduce linewidths to the order of millihertz.

A more exotic prospect is to take advantage of recent advances in Floquet engineering[70,71] to develop a diamond-based Floquet maser. Working with a ^{129}Xe vapor cell, a recent work by Jiang *et al.*[72] has demonstrated that it is possible to operate a maser based on transitions between Floquet states stabilized by an oscillating magnetic field $B_{ac}(t) = B\cos(\omega_{ac})$ that periodically drives the Zeeman sub-levels of the ^{129}Xe nuclear spins. The Floquet states $|\pm\rangle_n$ appear as sidebands offset from a central Larmor frequency ω_0 by integer-multiples of the driving frequency (i.e., at $\omega_0 \pm \omega_{ac}$), and population inversion into a majority $|+\rangle_n$ state is driven by spin-exchange collisions with a small admixture of optically pumped ^{87}Rb atoms. In place of a resonant cavity, the spin polarization is monitored directly via optical rotation of a probe laser and used to drive a feedback field B_f. In this way, it is possible to generate steady-state superradiant emission from the transition between $|+\rangle_n$ and $|-\rangle_n$ Floquet states. Such a maser can be used as a magnetometer where the field to be measured is used as the driving field, so that its amplitude and frequency may be determined by the properties of the Floquet sidebands. Interestingly, such a magnetometer appears to have a sensitivity that increases as the frequency of the measured field decreases, in contrast to SQUID magnetometers whose low-frequency response is hampered by $1/f$ noise. The sensitivity of the ^{129}Xe Floquet maser is limited to $\sim$700 fT/Hz$^{1/2}$ at 60 mHz due to field fluctuations from the ^{87}Rb atoms used to achieve inversion, though if these fluctuations can be overcome, it is expected that greater sensitivity can be achieved at even lower frequencies. It is here that a Floquet maser based on spin defects might offer an advantage through the relative ease with which they may be driven into specific quantum states.

An alternative approach to developing further solid-state room-temperature masers is to explore different gain media. As new host materials for spin defects are explored[73,74] and control over defect implantation improves, we anticipate that further defect-based room-temperature masers will emerge. Significant progress has already been made in this regard using silicon vacancies (V_{Si}) in silicon carbide (SiC), whose $S = 3/2$ ground state may be spin-polarized via intersystem crossing through optical pumping at $\sim$800 nm. Previous work[75] has demonstrated $T_2 \sim 100\ \mu$s coherence times and achieved population inversion leading to continuous microwave emission at room temperature, but in systems explored so far the gain factors have not exceeded losses in the cavity. A recent work by Fischer *et al.*[76] has explored in detail the conditions under which a continuous-wave maser using SiC as a gain medium at room temperature might be realized. It is convenient here to express the masing condition in terms of the gain medium quality factor[77]

$$Q_m = -\frac{\Delta\nu}{2K\mathcal{N}\beta^2\eta\Delta p}, \tag{1}$$

where $\Delta\nu$ is the resonance linewidth of the gain medium, $\mathcal{N}$ is the defect volume density, β^2 is the matrix element for the transition, η is the cavity filling factor, Δp is the population difference between the lower and higher energy level (taken by Fischer *et al.* to be -1.5%), and K is a constant equal to $g_e^2\mu_B^2\mu_0/h$. The condition for masing is then simply that the cavity quality factor should be greater than the gain medium quality factor $Q_c > Q_m$.

A further requirement is that the pump power required to achieve a population inversion should not heat the system to an extent that degrades its performance as a gain medium, determined to be $\sim$30 W/cm^2 for SiC. Fischer *et al.* estimate the necessary pump power in a cylindrical cavity of radius r and length L as

$$P \approx \frac{\pi r^2}{2}\tilde{P}_0 \exp\left(\frac{\mathcal{N}\sigma L}{2}\right), \tag{2}$$

where $\tilde{P}_0 = 3.9$ W/cm^2 is a characteristic pump power for SiC and $\sigma = 6.1 \times 10^{-15}$ cm^2 is the mean absorption cross section of the defects in their SiC sample. Since $\mathcal{N}$ is a common parameter of the two conditions, it must be carefully tuned to minimize Q_m while keeping $P < 30$ W/cm^2.

Using the sample parameters obtained from the sample of Fischer *et al.* and assuming a cavity with $Q_c \approx 2 \times 10^5$, we, therefore, expect masing to occur for 6.0×10^{14} cm$^{-3} < \mathcal{N} < 2.3 \times 10^{15}$ cm^{-3}. The upper bound on the defect density may be increased further to 9.2×10^{16} if the mean absorption cross section of defects in the system can be brought closer to the $\sigma \approx 1.5 \times 10^{-16}$ observed for individual V_{Si} defects.[78] The excess cross section is presumed to come from other types of defects such as neutral divacancies, so deterministic defect-implantation methods[79–81] should be able to achieve this by decreasing the relative concentrations of non-V_{Si} defects.

Since the defect densities required are within the range of densities that have already been achieved experimentally,[82] it seems that continuous-wave SiC masers that operate at room temperature are within reach.

Another host for spin defects that have shown promise is the van der Waals crystal hexagonal boron nitride (hBN), in which ensembles of negatively charged boron vacancies (V_B^-) with $S = 1$ have been successfully prepared in coherent quantum states with $T_2 \approx 10\,\mu$s spin coherence times at room temperature using optically-detected magnetic resonance (ODMR).[83–86] While the exact decoherence mechanism is not yet well understood, experimental[87] and theoretical[88] works suggest that the spin coherence time can be significantly improved by increasing the relative concentrations of ^{10}B (with nuclear spin $I = 3$) with respect to ^{11}B ($I = 3/2$), so that isotopically purified hBN might extend the range of defect-based gain media for room-temperature masers to include 2D materials. If significant population inversions and masing can be achieved for hBN, it will form an attractive system for low-volume, low-power devices analogous to nanolasers based on transition metal dichalcogenides.[89] The very large Stark shifts observed for defects in hBN[90] further offer the enticing possibility that the maser frequency in such devices could be tuned using electric fields and eliminate the need for magnetic fields altogether.

Aside from spin defects, an interesting recent proposal suggests that hydrogenic bound states of electrons and holes in semiconductors, known as Rydberg excitons, could form the basis of an electrically tunable continuous-wave maser[91] comparable to atomic Rydberg masers.[92] Rydberg states with a large principal quantum number n can be long-lived since their lifetime scales as n^2, though the $\sim n^{-3}$ energy difference between successive states typically makes it difficult to resolve high-n Rydberg excitons experimentally. For the semiconducting copper oxide Cu_2O, however, it has been possible[93] to observe excitons excited up to $n = 25$. Ziemkiewicz and Zielínska-Raczýnska propose that by placing a mm-sized sample of Cu_2O in a cavity and using the Stark shifts induced by an external electric field to match the transition between different Rydberg states to a 571 nm optical pump, it will be possible to selectively pump between specific Rydberg states. There are 2300 three-level subsets $\{n_1, n_2, n_3\}$ that can be selected from the 25 available Rydberg states, allowing the maser transition to be broadly tuned over wavelengths from 0.1–10 mm. Although milliKelvin temperatures are required to access the 25 Rydberg states modeled by Ziemkiewicz and Zielínska-Raczýnska, it will be interesting to explore whether this approach can be realized at room temperature. Recent work[94] on synthetic Cu_2O with very low levels of defects and impurities reported the observation of excitonic Rydberg states at room temperature. Aside from Cu_2O, room-temperature Rydberg states up to $n = 4$ have also been observed in monolayers of transition metal dichalcogenides such as MoS_2 and WS_2.[95] These would provide another route to a two-dimensional room-temperature nanomaser.

As the range of gain media and operating principles for room-temperature solid-state masers continues to grow, it is interesting finally to speculate what applications might open up as practical devices become available. Masers have historically been important in metrology, where their ultra-low-noise amplification has allowed the detection of very weak electromagnetic signals. For this reason, we anticipate that room-temperature masers will find ready use in deep-space communications and as sensitive magnetometers. For the latter, the diamond maser has already shown sensitivities of order 10 pT/$\sqrt{\text{Hz}}$ and might be made more sensitive still by masing between Floquet states, as discussed above.

Another prominent application of masers has been as frequency standards[18] with the hydrogen maser recently employed in the Galileo[96] and BeiDou[97] satellite navigation systems. An attractive use for masers that operate at ambient temperature and pressure might, therefore, be as highly portable precision clocks that could maintain local synchronization with a satellite navigation system when satellite signals are obstructed. Over short (seconds to minutes) timescale clock stability is largely determined by the clock signal Q factor, so we may expect the diamond maser ($Q \sim 10^8$–10^{11}) to be highly competitive with quartz resonators ($Q \sim 10^6$ and with non-masing diamond NV center clocks ($Q \sim 100$) based on zero-field transitions between the $|\pm 1\rangle$ and $|0\rangle$ ground states.[98] The key challenge to realizing a practical chip-based diamond maser clock will lie in overcoming the sensitivity to temperature fluctuations either by employing one of the alternative maser operating principles discussed above or by introducing ways to compensate the temperature-dependence of the masing frequency.[98]

We further anticipate that the arrival of masers that operates in ambient conditions will extend the benefits of lasers in spectroscopy (e.g., low linewidths and high spatial coherence) to microwave wavelengths, leading to new developments in microwave spectroscopy[99,100] and sensing applications.[101] A key step in this direction will be to increase the output power that can be achieved by room-temperature solid-state masers.

It is finally interesting to speculate whether room-temperature masers may contribute to the suite of applications in quantum technology currently being explored more generally for spin defects in wide-bandgap materials.[102–104] The observation of strong coupling and highly entangled Dicke states in the pentacene maser are promising in this regard[105] with Dicke states playing an important role in quantum metrology[106,107] and quantum computing.[108,109] Alternatively, the coherent radiation generated using room-temperature solid state masers might be employed[110] in microwave quantum illumination systems[111,112] to achieve a form of quantum radar that uses photon correlations to outperform classical systems in the detection of low-reflectivity targets in a noisy environment.[113] Finally, the formal analogy between three-level masers and heat engines[114] suggests that solid-state room-temperature masers may be employed as quantum heat engines, whose coherence enables them to deliver a greater power output than their classical counterparts.[115] A population-inverted diamond NV center system was recently operated as a quantum heat engine to demonstrate that such quantum advantages can be realized experimentally.[116]

Room-temperature solid state masers, thus, offer attractive systems with which to explore fundamental questions in quantum optics as well as challenges in metrology and quantum technologies. In the coming years, we expect to see ever more materials and device concepts exploited to further develop masers and address these challenges.

ACKNOWLEDGMENTS

This work was supported by the Royal Society and the UK Engineering and Physical Sciences Research Council (No. EP/S000798/1). We also acknowledge support from the Henry Royce Institute.

DATA AVAILABILITY

The data that support the findings of this study are available from the corresponding author upon reasonable request.

REFERENCES

[1]J. Weber, "Amplification of microwave radiation by substances not in thermal equilibrium," Trans. IRE Prof. Group Electron Devices **PGED-3**, 1–4 (1953).
[2]N. Basov and A. Prokhorov, "About possible methods for obtaining active molecules for a molecular oscillator," J. Exp. Theor. Phys. **1**, 185 (1955).
[3]J. P. Gordon, H. J. Zeiger, and C. H. Townes, "Molecular microwave oscillator and new hyperfine structure in the microwave spectrum of NH_3," Phys. Rev. **95**, 282 (1954).
[4]H. M. Goldenberg, D. Kleppner, and N. F. Ramsey, "Atomic hydrogen maser," Phys. Rev. Lett. **5**, 361–362 (1960).
[5]D. Kleppner, H. M. Goldenberg, and N. F. Ramsey, "Theory of the hydrogen maser," Phys. Rev. **126**, 603–615 (1962).
[6]N. Bloembergen, "Proposal for a new type solid state maser," Phys. Rev. **104**, 324–327 (1956).
[7]H. E. D. Scovil, G. Feher, and H. Seidel, "Operation of a solid state maser," Phys. Rev. **105**, 762–763 (1957).
[8]A. L. McWhorter and J. W. Meyer, "Solid-state maser amplifier," Phys. Rev. **109**, 312–318 (1958).
[9]G. Makhov, C. Kikuchi, J. Lambe, and R. W. Terhune, "Maser action in ruby," Phys. Rev. **109**, 1399–1400 (1958).
[10]R. W. DeGrasse, E. O. Schulz-Dubois, and H. E. D. Scovil, "The three-level solid state traveling-wave maser," Bell Syst. Tech. J. **38**, 305–334 (1959).
[11]R. Forward, F. Goodwin, and J. Kiefer, "Application of a solid-state ruby maser to an x-band radar system," in *WESCON/59 Conference Record* (IEEE, 1959), Vol. 3, pp. 119–125.
[12]R. Price, P. E. Green, T. J. Goblick, R. H. Kingston, L. G. Kraft, G. H. Pettengill, R. Silver, and W. B. Smith, "Radar echoes from venus," Science **129**, 751–753 (1959).
[13]J. A. Giordmaine, "Microwave spectroscopy, the maser, and radio astronomy: Charles Townes at Columbia," in *Amazing Light: A Volume Dedicated to Charles Hard Townes on His 80th Birthday*, edited by R. Y. Chiao (Springer, New York, 1996), pp. 273–275.
[14]T. H. Maiman, "Stimulated optical radiation in ruby," Nature **187**, 493–494 (1960).
[15]D. Kleppner, H. M. Goldenberg, and N. F. Ramsey, "Properties of the hydrogen maser," Appl. Opt. **1**, 55–60 (1962).
[16]I. Konoplev, P. McGrane, W. He, A. Cross, A. Phelps, C. Whyte, K. Ronald, and C. Robertson, "Experimental study of coaxial free-electron maser based on two-dimensional distributed feedback," Phys. Rev. Lett. **96**, 035002 (2006).
[17]A. E. Siegman, *Microwave Solid-State Masers* (McGraw-Hill, 1964).
[18]M. A. Lombardi, "Time and frequency," in *Encyclopedia of Physical Science and Technology*, 3rd ed., edited by R. A. Meyers (Academic Press, Cambridge, MA, 2003), pp. 783–801.
[19]L. Coldren, S. Corzine, and M. Mashanovitch, *Diode Lasers and Photonic Integrated Circuits*, Wiley Series in Microwave and Optical Engineering (Wiley, 2012).
[20]A. R. Lepley and G. L. Closs, *Chemically Induced Magnetic Polarization* (Wiley-Interscience, 1973).
[21]A. Kastler, "Optical methods for studying Hertzian resonances," Science **158**, 214–221 (1967).
[22]E. Mattison, R. Vessot, and W. Shen, "Single-state selection system for hydrogen masers," IEEE Trans. Ultrasonics, Ferroelectr., Freq. Control **34**, 622–628 (1987).
[23]A. Barannik, N. Cherpak, A. Kirichenko, Y. Prokopenko, S. Vitusevich, and V. Yakovenko, "Whispering gallery mode resonators in microwave physics and technologies," Int. J. Microwave Wireless Technol. **9**, 781–796 (2017).
[24]P.-Y. Bourgeois, N. Bazin, Y. Kersalé, V. Giordano, M. Tobar, and M. Oxborrow, "Maser oscillation in a whispering-gallery-mode microwave resonator," Appl. Phys. Lett. **87**, 224104 (2005).
[25]D. L. Creedon, K. Benmessai, M. E. Tobar, J. G. Hartnett, P.-Y. Bourgeois, Y. Kersale, J.-M. L. Floch, and V. Giordano, "High power solid-state sapphire whispering gallery mode maser," in *IEEE International Frequency Control Symposium Joint with the 22nd European Frequency and Time Forum* (IEEE, 2009), pp. 282–285.
[26]K. Benmessaï, P.-Y. Bourgeois, M. E. Tobar, N. Bazin, Y. Kersalé, and V. Giordano, "Amplification process in a high-Q cryogenic whispering gallery mode sapphire Fe^{3+} maser," Meas. Sci. Technol. **21**, 025902 (2010).
[27]K. Benmessai, D. L. Creedon, M. E. Tobar, P.-Y. Bourgeois, Y. Kersalé, and V. Giordano, "Measurement of the fundamental thermal noise limit in a cryogenic sapphire frequency standard using bimodal maser oscillations," Phys. Rev. Lett. **100**, 233901 (2008).
[28]A. L. Schawlow and C. H. Townes, "Infrared and optical masers," Phys. Rev. **112**, 1940–1949 (1958).
[29]M. Oxborrow, J. D. Breeze, and N. M. Alford, "Room-temperature solid-state maser," Nature **488**, 353–356 (2012).
[30]C. A. Flory and R. Taber, "High performance distributed Bragg reflector microwave resonator," IEEE Trans. Ultrasonics, Ferroelectr., Freq. Control **44**, 486–495 (1997).
[31]J. Breeze, J. Krupka, and N. M. Alford, "Enhanced quality factors in aperiodic reflector resonators," Appl. Phys. Lett. **91**, 152902 (2007).
[32]J. Breeze, M. Oxborrow, and N. M. Alford, "Better than Bragg: Optimizing the quality factor of resonators with aperiodic dielectric reflectors," Appl. Phys. Lett. **99**, 113515 (2011).
[33]E. Brock, P. Csavinszky, E. Hormats, H. Nedderman, D. Stirpe, and F. Unterleitner, "Coherent stimulated emission from organic molecular crystals," J. Chem. Phys. **35**, 759–760 (1961).
[34]A. Blank, R. Kastner, and H. Levanon, "Exploring new active materials for low-noise room-temperature microwave amplifiers and other devices," IEEE Trans. Microwave Theory Tech. **46**, 2137–2144 (1998).
[35]A. Blank and H. Levanon, "Applications of photoinduced electron spin polarization at room temperature to microwave technology," Appl. Phys. Lett. **79**, 1694–1696 (2001).
[36]A. Blank and H. Levanon, "Toward maser action at room temperature by triplet-radical interaction and its application to microwave technology," RIKEN Rev. **44**, 128–130 (2002).
[37]C. Blättler, F. Jent, and H. Paul, "A novel radical-triplet pair mechanism for chemically induced electron polarization (CIDEP) of free radicals in solution," Chem. Phys. Lett. **166**, 375–380 (1990).
[38]D. J. Sloop, H.-L. Yu, T.-S. Lin, and S. Weissman, "Electron spin echoes of a photoexcited triplet: Pentacene in p-terphenyl crystals," J. Chem. Phys. **75**, 3746–3757 (1981).
[39]J. D. Breeze, E. Salvadori, J. Sathian, N. M. Alford, and C. W. Kay, "Room-temperature cavity quantum electrodynamics with strongly coupled Dicke states," npj Quantum Inf. **3**, 40 (2017).
[40]J. Breeze, K.-J. Tan, B. Richards, J. Sathian, M. Oxborrow, and N. M. Alford, "Enhanced magnetic Purcell effect in room-temperature masers," Nat. Commun. **6**, 6215 (2015).
[41]E. M. Purcell, "Spontaneous emission probabilities at radio frequencies," Phys. Rev. **69**, 674–674 (1946).
[42]E. Salvadori, J. D. Breeze, K.-J. Tan, J. Sathian, B. Richards, M. W. Fung, G. Wolfowicz, M. Oxborrow, N. M. Alford, and C. W. Kay, "Nanosecond time-resolved characterization of a pentacene-based room-temperature MASER," Sci. Rep. **7**, 41836 (2017).
[43]N. P. Fokina and M. O. Elizbarashvili, "Pure superradiance from the inverted levels of spin triplet states coupled to resonator," Appl. Magn. Reson. **52**, 769 (2021).
[44]H. Wu, X. Xie, W. Ng, S. Mehanna, Y. Li, M. Attwood, and M. Oxborrow, "Room-temperature quasi-continuous-wave pentacene maser pumped by an invasive Ce:YAG luminescent concentrator," Phys. Rev. Appl. **14**, 064017 (2020).

[45]H. Wu, W. Ng, S. Mirkhanov, A. Amirzhan, S. Nitnara, and M. Oxborrow, "Unraveling the room-temperature spin dynamics of photoexcited pentacene in its lowest triplet state at zero field," J. Phys. Chem. C **123**, 24275–24279 (2019).
[46]S. Bogatko, P. D. Haynes, J. Sathian, J. Wade, J.-S. Kim, K.-J. Tan, J. Breeze, E. Salvadori, A. Horsfield, and M. Oxborrow, "Molecular design of a room-temperature maser," J. Phys. Chem. C **120**, 8251–8260 (2016).
[47]J. R. Weber, W. F. Koehl, J. B. Varley, A. Janotti, B. B. Buckley, C. G. Van de Walle, and D. D. Awschalom, "Quantum computing with defects," Proc. Natl. Acad. Sci. **107**, 8513–8518 (2010).
[48]J. Loubser and J. Van Wyk, "Optical spin-polarisation in a triplet state in irradiated and annealed type 1b diamonds," Diamond Res. **1977**, 11–14.
[49]L. Jin, M. Pfender, N. Aslam, P. Neumann, S. Yang, J. Wrachtrup, and R.-B. Liu, "Proposal for a room-temperature diamond maser," Nat. Commun. **6**, 8251 (2015).
[50]J. D. Breeze, E. Salvadori, J. Sathian, N. M. Alford, and C. W. Kay, "Continuous-wave room-temperature diamond maser," Nature **555**, 493–496 (2018).
[51]A. Sherman, L. Buchbinder, S. Ding, and A. Blank, "Performance analysis of diamond-based masers," J. Appl. Phys. **129**, 144503 (2021).
[52]A. Wickenbrock, H. Zheng, G. Chatzidrosos, J. Shaji Rebeirro, T. Schneemann, and P. Blümler, "High homogeneity permanent magnet for diamond magnetometry," J. Magn. Reson. **322**, 106867 (2021).
[53]J. F. Barry, J. M. Schloss, E. Bauch, M. J. Turner, C. A. Hart, L. M. Pham, and R. L. Walsworth, "Sensitivity optimization for NV-diamond magnetometry," Rev. Mod. Phys. **92**, 015004 (2020).
[54]E. Bauch, S. Singh, J. Lee, C. A. Hart, J. M. Schloss, M. J. Turner, J. F. Barry, L. M. Pham, N. Bar-Gill, S. F. Yelin, and R. L. Walsworth, "Decoherence of ensembles of nitrogen-vacancy centers in diamond," Phys. Rev. B **102**, 134210 (2020).
[55]M. O. Scully and M. Fleischhauer, "Lasers without inversion," Science **263**, 337–338 (1994).
[56]J. Mompart and R. Corbalan, "Lasing without inversion: Realities and prospects," Proc. SPIE **3572**, 33–44 (1999).
[57]A. Mysyrowicz, R. Danylo, A. Houard, V. Tikhonchuk, X. Zhang, Z. Fan, Q. Liang, S. Zhuang, L. Yuan, and Y. Liu, "Lasing without population inversion in N_2^+," APL Photonics **4**, 110807 (2019).
[58]C. Ott, A. Kaldun, P. Raith, K. Meyer, M. Laux, J. Evers, C. H. Keitel, C. H. Greene, and T. Pfeifer, "Lorentz meets fano in spectral line shapes: A universal phase and its laser control," Science **340**, 716–720 (2013).
[59]A. S. Zibrov, M. D. Lukin, D. E. Nikonov, L. Hollberg, M. O. Scully, V. L. Velichansky, and H. G. Robinson, "Experimental demonstration of laser oscillation without population inversion via quantum interference in Rb," Phys. Rev. Lett. **75**, 1499–1502 (1995).
[60]E. S. Fry, X. Li, D. Nikonov, G. G. Padmabandu, M. O. Scully, A. V. Smith, F. K. Tittel, C. Wang, S. R. Wilkinson, and S.-Y. Zhu, "Atomic coherence effects within the sodium d_1 line: Lasing without inversion via population trapping," Phys. Rev. Lett. **70**, 3235–3238 (1993).
[61]C. Santori, D. Fattal, S. M. Spillane, M. Fiorentino, R. G. Beausoleil, A. D. Greentree, P. Olivero, M. Draganski, J. R. Rabeau, P. Reichart, B. C. Gibson, S. Rubanov, D. N. Jamieson, and S. Prawer, "Coherent population trapping in diamond n-v centers at zero magnetic field," Opt. Express **14**, 7986–7994 (2006).
[62]M. Gross and S. Haroche, "Superradiance: An essay on the theory of collective spontaneous emission," Phys. Rep. **93**, 301–396 (1982).
[63]R. H. Dicke, "Coherence in spontaneous radiation processes," Phys. Rev. **93**, 99–110 (1954).
[64]K. Hepp and E. H. Lieb, "On the superradiant phase transition for molecules in a quantized radiation field: The Dicke maser model," Ann. Phys. **76**, 360–404 (1973).
[65]D. Meiser, J. Ye, D. R. Carlson, and M. J. Holland, "Prospects for a millihertz-linewidth laser," Phys. Rev. Lett. **102**, 163601 (2009).
[66]J. G. Bohnet, Z. Chen, J. M. Weiner, D. Meiser, M. J. Holland, and J. K. Thompson, "A steady-state superradiant laser with less than one intracavity photon," Nature **484**, 78–81 (2012).
[67]S. Putz, D. O. Krimer, R. Amsüss, A. Valookaran, T. Nöbauer, J. Schmiedmayer, S. Rotter, and J. Majer, "Protecting a spin ensemble against decoherence in the strong-coupling regime of cavity QED," Nat. Phys. **10**, 720–724 (2014).
[68]A. Angerer, K. Streltsov, T. Astner, S. Putz, H. Sumiya, S. Onoda, J. Isoya, W. J. Munro, K. Nemoto, J. Schmiedmayer, and J. Majer, "Superradiant emission from colour centres in diamond," Nat. Phys. **14**, 1168–1172 (2018).
[69]Q. Wu, Y. Zhang, X. Yang, S.-L. Su, C. Shan, and K. Mølmer, "A superradiant maser with nitrogen-vacancy center spins," arXiv:2105.12350 (2021).
[70]R. Moessner and S. L. Sondhi, "Equilibration and order in quantum floquet matter," Nat. Phys. **13**, 424–428 (2017).
[71]T. Oka and S. Kitamura, "Floquet engineering of quantum materials," Annu. Rev. Condens. Matter Phys. **10**, 387–408 (2019).
[72]M. Jiang, H. Su, Z. Wu, X. Peng, and D. Budker, "Floquet maser," Sci. Adv. **7**, eabe0719 (2021).
[73]L. C. Bassett, A. Alkauskas, A. L. Exarhos, and K.-M. C. Fu, "Quantum defects by design," Nanophotonics **8**, 1867–1888 (2019).
[74]G. Wolfowicz, F. J. Heremans, C. P. Anderson, S. Kanai, H. Seo, A. Gali, G. Galli, and D. D. Awschalom, "Quantum guidelines for solid-state spin defects," Nat. Rev. Mater. **6**, 906–925 (2021).
[75]H. Kraus, V. Soltamov, D. Riedel, S. Väth, F. Fuchs, A. Sperlich, P. Baranov, V. Dyakonov, and G. Astakhov, "Room-temperature quantum microwave emitters based on spin defects in silicon carbide," Nat. Phys. **10**, 157–162 (2014).
[76]M. Fischer, A. Sperlich, H. Kraus, T. Ohshima, G. Astakhov, and V. Dyakonov, "Highly efficient optical pumping of spin defects in silicon carbide for stimulated microwave emission," Phys. Rev. Appl. **9**, 054006 (2018).
[77]A. E. Siegman, *Microwave Solid-State Masers* (McGraw-Hill, 1964), p. 255.
[78]F. Fuchs, B. Stender, M. Trupke, D. Simin, J. Pflaum, V. Dyakonov, and G. V. Astakhov, "Engineering near-infrared single-photon emitters with optically active spins in ultrapure silicon carbide," Nat. Commun. **6**, 7578 (2015).
[79]J. Wang, Y. Zhou, X. Zhang, F. Liu, Y. Li, K. Li, Z. Liu, G. Wang, and W. Gao, "Efficient generation of an array of single silicon-vacancy defects in silicon carbide," Phys. Rev. Appl. **7**, 064021 (2017).
[80]J.-F. Wang, Q. Li, F.-F. Yan, H. Liu, G.-P. Guo, W.-P. Zhang, X. Zhou, L.-P. Guo, Z.-H. Lin, J.-M. Cui, X.-Y. Xu, J.-S. Xu, C.-F. Li, and G.-C. Guo, "On-demand generation of single silicon vacancy defects in silicon carbide," ACS Photonics **6**, 1736–1743 (2019).
[81]Y.-C. Chen, P. S. Salter, M. Niethammer, M. Widmann, F. Kaiser, R. Nagy, N. Morioka, C. Babin, J. Erlekampf, P. Berwian, M. J. Booth, and J. Wrachtrup, "Laser writing of scalable single color centers in silicon carbide," ACS Nano Lett. **19**, 2377–2383 (2019).
[82]F. Fuchs, "Optical spectroscopy on silicon vacancy defects in silicon carbide," Ph.D. thesis (Universität Würzburg, 2015).
[83]A. Gottscholl, M. Kianinia, V. Soltamov, S. Orlinskii, G. Mamin, C. Bradac, C. Kasper, K. Krambrock, A. Sperlich, M. Toth, I. Aharonovich, and V. Dyakonov, "Initialization and read-out of intrinsic spin defects in a van der waals crystal at room temperature," Nat. Mater. **19**, 540–545 (2020).
[84]M. Kianinia, S. White, J. E. Fröch, C. Bradac, and I. Aharonovich, "Generation of spin defects in hexagonal boron nitride," ACS Photonics **7**, 2147–2152 (2020).
[85]H. L. Stern, J. Jarman, Q. Gu, S. E. Barker, N. Mendelson, D. Chugh, S. Schott, H. H. Tan, H. Sirringhaus, I. Aharonovich, and M. Atatüre, "Room-temperature optically detected magnetic resonance of single defects in hexagonal boron nitride," arXiv:2103.16494 (2021).
[86]N. Chejanovsky, A. Mukherjee, J. Geng, Y.-C. Chen, Y. Kim, A. Denisenko, A. Finkler, T. Taniguchi, K. Watanabe, D. B. R. Dasari, P. Auburger, A. Gali, J. H. Smet, and J. Wrachtrup, "Single-spin resonance in a van der Waals embedded paramagnetic defect," Nat. Mater. **20**, 1079 (2021).
[87]A. Gottscholl, M. Diez, V. Soltamov, C. Kasper, A. Sperlich, M. Kianinia, C. Bradac, I. Aharonovich, and V. Dyakonov, "Room temperature coherent control of spin defects in hexagonal boron nitride," Sci. Adv. **7**, eabf3630 (2021).
[88]M. Ye, H. Seo, and G. Galli, "Spin coherence in two-dimensional materials," npj Comput. Mater. **5**, 44 (2019).
[89]Y. Li, J. Zhang, D. Huang, H. Sun, F. Fan, J. Feng, Z. Wang, and C. Z. Ning, "Room-temperature continuous-wave lasing from monolayer molybdenum ditelluride integrated with a silicon nanobeam cavity," Nat. Nanotechnol. **12**, 987–992 (2017).

[90]Y. Xia, Q. Li, J. Kim, W. Bao, C. Gong, S. Yang, Y. Wang, and X. Zhang, "Room-temperature giant Stark effect of single photon emitter in van der Waals material," Nano Lett. **19**, 7100–7105 (2019).
[91]D. Ziemkiewicz and S. Zielińska-Raczyńska, "Proposal of tunable Rydberg exciton maser," Opt. Lett. **43**, 3742–3745 (2018).
[92]L. Moi, P. Goy, M. Gross, J. M. Raimond, C. Fabre, and S. Haroche, "Rydberg-atom masers. I. A theoretical and experimental study of super-radiant systems in the millimeter-wave domain," Phys. Rev. A **27**, 2043 (1983).
[93]T. Kazimierczuk, D. Fröhlich, S. Scheel, H. Stolz, and M. Bayer, "Giant Rydberg excitons in the copper oxide Cu_2O," Nature **514**, 343–347 (2014).
[94]S. Steinhauer, M. A. M. Versteegh, S. Gyger, A. W. Elshaari, B. Kunert, A. Mysyrowicz, and V. Zwiller, "Rydberg excitons in Cu_2O microcrystals grown on a silicon platform," Commun. Mater. **1**, 11 (2020).
[95]H. M. Hill, A. F. Rigosi, C. Roquelet, A. Chernikov, T. C. Berkelbach, D. R. Reichman, M. S. Hybertsen, L. E. Brus, and T. F. Heinz, "Observation of excitonic Rydberg states in monolayer MoS_2 and WS_2 by photoluminescence excitation spectroscopy," Nano Lett. **15**, 2992–2997 (2015).
[96]F. Droz, P. Mosset, G. Barmaverain, P. Rochat, Q. Wang, M. Belloni, L. Mattioni, U. Schmidt, T. Pike, F. Emma, and P. Waller, "The on-board Galileo clocks: Rubidium standard and passive hydrogen maser—current status and performance," in *Proceedings of the 20th European Frequency and Time Forum* (European Frequency and Time Forum, 2006), pp. 420–426.
[97]J. Li, J. Zhang, Y. Bu, C. Cao, W. Wang, and H. Zheng, "Space passive hydrogen maser a passive hydrogen maser for space applications," in *IEEE International Frequency Control Symposium (IFCS)* (IEEE, 2016), pp. 1–5.
[98]J. S. Hodges, N. Y. Yao, D. Maclaurin, C. Rastogi, M. D. Lukin, and D. Englund, "Timekeeping with electron spin states in diamond," Phys. Rev. A **87**, 032118 (2013).
[99]J. F. Ready, "Laser applications in spectroscopy," in *Industrial Applications of Lasers*, 2nd ed., edited by J. F. Ready (Academic Press, San Diego, 1997), Chap. 20, pp. 491–509.
[100]L. Li, M. Sun, X.-H. Li, Z.-W. Zhao, H.-M. Ma, H.-Y. Gan, Z.-H. Lin, S.-C. Shi, and L. M. Ziurys, "Recent advances on rotational spectroscopy and microwave spectroscopic techniques," Chin. J. Anal. Chem. **42**, 1369–1378 (2014).
[101]F. Li, Y. Zheng, C. Hua, and J. Jian, "Gas sensing by microwave transduction: Review of progress and challenges," Front. Mater. **6**, 101 (2019).
[102]N. T. Son, C. P. Anderson, A. Bourassa, K. C. Miao, C. Babin, M. Widmann, M. Niethammer, J. Ul Hassan, N. Morioka, I. G. Ivanov, F. Kaiser, J. Wrachtrup, and D. D. Awschalom, "Developing silicon carbide for quantum spintronics," Appl. Phys. Lett. **116**, 190501 (2020).
[103]S. Pezzagna and J. Meijer, "Quantum computer based on color centers in diamond," Appl. Phys. Rev. **8**, 011308 (2021).
[104]M. Ruf, N. H. Wan, H. Choi, D. Englund, and R. Hanson, "Quantum networks based on color centers in diamond," arXiv:2105.04341 (2021).
[105]R. Amsüss, C. Koller, T. Nöbauer, S. Putz, S. Rotter, K. Sandner, S. Schneider, M. Schramböck, G. Steinhauser, H. Ritsch, J. Schmiedmayer, and J. Majer, "Cavity QED with magnetically coupled collective spin states," Phys. Rev. Lett. **107**, 060502 (2011).
[106]O. Hosten, R. Krishnakumar, N. J. Engelsen, and M. A. Kasevich, "Quantum phase magnification," Science **352**, 1552–1555 (2016).
[107]G. Tóth, "Multipartite entanglement and high-precision metrology," Phys. Rev. A **85**, 022322 (2012).
[108]P. Rotondo, M. Cosentino Lagomarsino, and G. Viola, "Dicke simulators with emergent collective quantum computational abilities," Phys. Rev. Lett. **114**, 143601 (2015).
[109]R. Prevedel, G. Cronenberg, M. S. Tame, M. Paternostro, P. Walther, M. S. Kim, and A. Zeilinger, "Experimental realization of Dicke states of up to six qubits for multiparty quantum networking," Phys. Rev. Lett. **103**, 020503 (2009).
[110]A. Karsa and S. Pirandola, "Classical benchmarking for microwave quantum illumination," arXiv:2105.04527 (2021).
[111]S. Barzanjeh, S. Guha, C. Weedbrook, D. Vitali, J. H. Shapiro, and S. Pirandola, "Microwave quantum illumination," Phys. Rev. Lett. **114**, 080503 (2015).
[112]S. Barzanjeh, S. Pirandola, D. Vitali, and J. M. Fink, "Microwave quantum illumination using a digital receiver," Sci. Adv. **6**, eabb0451 (2020).
[113]S.-H. Tan, B. I. Erkmen, V. Giovannetti, S. Guha, S. Lloyd, L. Maccone, S. Pirandola, and J. H. Shapiro, "Quantum illumination with Gaussian states," Phys. Rev. Lett. **101**, 253601 (2008).
[114]H. E. D. Scovil and E. O. Schulz-DuBois, "Three-level masers as heat engines," Phys. Rev. Lett. **2**, 262–263 (1959).
[115]R. Uzdin, A. Levy, and R. Kosloff, "Equivalence of quantum heat machines, and quantum-thermodynamic signatures," Phys. Rev. X **5**, 031044 (2015).
[116]J. Klatzow, J. N. Becker, P. M. Ledingham, C. Weinzetl, K. T. Kaczmarek, D. J. Saunders, J. Nunn, I. A. Walmsley, R. Uzdin, and E. Poem, "Experimental demonstration of quantum effects in the operation of microscopic heat engines," Phys. Rev. Lett. **122**, 110601 (2019).